ST-ECF Instrument Science Report WFC3-2011-05

Revised Flux Calibration of the WFC3 G102 and G141 grisms

H. Kuntschner, M. Kümmel, J. R. Walsh, H. Bushouse
January 11, 2011

ABSTRACT

Based on observations of the primary HST flux standard stars GD153 and GD71 (Programs 11552 and 11936), the flux calibration of the WFC3 IR G102 and G141 grisms is revised. With the new calibrations the total throughput of HST + WFC3 G102 peaks at 1100 nm with 41% and is above 10% between 804 and 1153 nm. For G141 the total throughput in the +1st order peaks at 48% and is above 10% between 1081 and 1691 nm. The accuracy of the absolute flux calibration for point sources is about 2% (one standard deviation) and better than 5% for most of the field-of-view.
We also provide revised aperture corrections for the +1st order as a function of wavelength for each grism and determine the large-scale throughput variations for the grisms as a function of the field-of-view.

1. Introduction

The Wide Field Camera 3 (WFC3) is fitted with three grisms for slitless spectroscopy. In the UVIS channel there is one grism, G280, for the near-UV to visible range (200 - 400nm). The NIR channel has two grisms, G102 and G141, for the shorter (800 - 1150nm) and longer NIR wavelengths (1100-1700nm), respectively. The first results from in-orbit calibrations including trace,

wavelength, throughput and aperture correction calibrations are summarized in Kuntschner et al. (2009a,b). This report presents updated in-orbit calibrations for the G102 and G141 grisms derived from SMOV and Cycle 17 calibration observations in Programs 11552 and 11936.

2. Observations

The calibrations presented in this report are based on the SMOV program 11552 (PI: Bushouse), which includes observations of the HST primary flux standard star GD153 at essentially 3 different positions over the field-of-view (hereafter FoV) for each grism. Furthermore, we made use of the Cycle 17 calibration program 11936 (PI: Bushouse), which includes observations of the HST primary flux standard star GD71 at 9 different field positions and two telescope orientations (~90˚ and ~275˚) for each grism. All grism observations are preceded by two direct images in (broadband) filters matching the grism wavelength; F098M and F105W for the G102 grism and F140W and F160W for the G141 grism.

3. Analysis

In this section we describe the revised flux calibrations, the aperture corrections and the large-scale throughput variations for the G102 and G141 grisms. Unless stated otherwise, analysis was carried out on fully processed images (i.e. "_flt.fits" files). The files were downloaded from the ST-ECF cache in December 2010, running the calwf3 pipeline version 2.1. Sky subtraction is achieved by making use of the global sky subtraction method using "Master-sky" images (see also Kümmel et al. 2011). Important improvements over previous analyses stem from the combination of improvements in calwf3, newer aXe software versions including bad pixel and cosmic ray rejection in the drizzling step, and more accurate background subtraction with the Master-sky. We also made use of new large-scale flat-field calibrations as documented in Section 3.3. Furthermore, the observations of GD71 in Cycle 17 enable verifying the flux calibration over 9 independent positions in the FoV. The observations of GD71 suffer from mild but noticeable spectral overlap by neighbouring, fainter stars and thus are not ideally suited to carry out a primary flux calibration. It is for this reason that we opted to use only the GD153 observations for the primary flux calibration of the WFC3 IR grisms.

3.1. Throughput measurements

Using the trace and wavelength solutions presented in previous ISRs (Kuntschner 2009a,b) the spectra of the flux standard star GD153 observed in Program 11552 were extracted. Note that we make use of our own flat-field calibrations (see also

Section 3.3; Kuntschner et al. 2008), which significantly improves the quality of the spectra. For each grism there are four slightly dithered exposures taken near the central position of the FoV. A further two exposures cover the top left and bottom right corners of the FoV. For the final flux calibration we combine the $+1^{st}$ order of the four central exposures into a single spectrum with the help of the spectral drizzle option in the aXe software (aXedrizzle; aXe version 2.1). Due to the superposition of several pixels marked in the DQ map as "hot" (DQ value 16) the drizzled spectra showed areas of unrealistically suppressed count levels. In order to circumvent this problem, all data in this report were reduced with a DQ mask value of 8454 (flags of 2, 4, 256, 8192; i.e. ignoring hot pixels) in the aXe configuration file. This procedure resulted in very well-defined spectra for the flux standard star.

Firstly, the spectrum, extracted over a width of 48 pixels (6.156 arcsec) was aperture corrected to infinity (see Section 3.2; 0.8% and 1.2% for the G102 and G141 grisms, respectively), then the spectrum was converted to units of [e^- / Å / sec] and divided by a smoothed version of the model spectrum taken from the HST CALSPEC library (gd153_mod_007.fits). Smoothing in a sliding 7-pixel window provides the final sensitivity function. The error is evaluated by taking the standard deviation of the four individual sensitivity curves from the central pointings at each wavelength bin and imposing a minimum error of 1%. Using this new sensitivity curve, Figure 1 shows for the G102 grism (from the top) the aXe-extracted spectra in electrons per second per pixel, in flux units and the ratio of the observed flux over the model spectrum versus wavelength. In the top plot of Figure 1, significant variations between spectra can be seen, because the spectral dispersion (Å/pixel) changes as a function of position within the field-of-view. The overall agreement between the fully calibrated standard star spectra (middle plot) is good for the wavelength range 790 to 1150 nm.

The spectrum coloured in red (bottom right field position) shows between 2 and 5% too much flux for wavelengths beyond 900 nm. Since this spectrum was not part of the flux calibration, this deviation indicates that the current large scale flat-field correction is slightly too large for this position in the FoV (for details of the large scale flat-field see Section 3.3).

An identical analysis was carried out for the G141 grism and results are shown in Figure 2. The overall agreement between the fully calibrated standard star spectra (middle plot) is excellent for the wavelength range 1075 to 1675 nm.

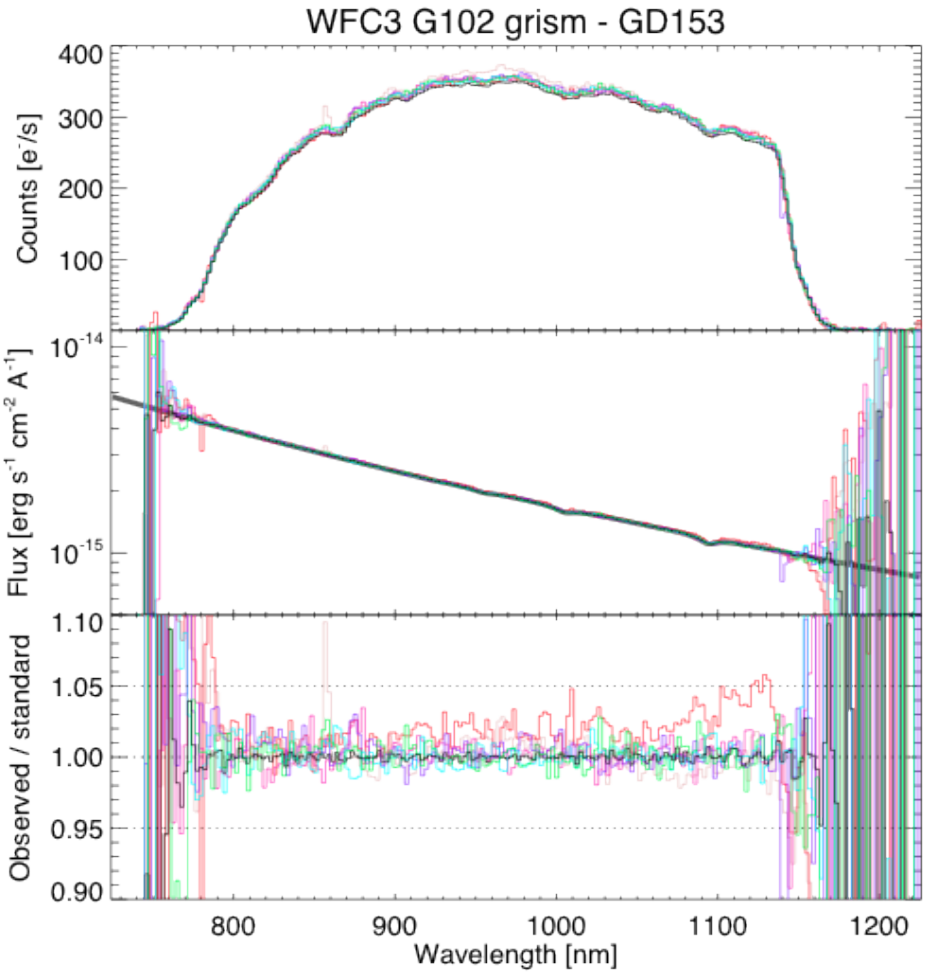

Figure 1: Flux calibration of the G102 grism. From top to bottom: The aXe extracted 1-dimensional spectra of the standard star GD153 in units of electrons per second per pixel, fully calibrated flux units and the ratio of the observed flux over the model spectrum versus wavelength. Observations obtained at different field positions are coloured, and the combined (aXedrizzle) central spectrum is shown in black.

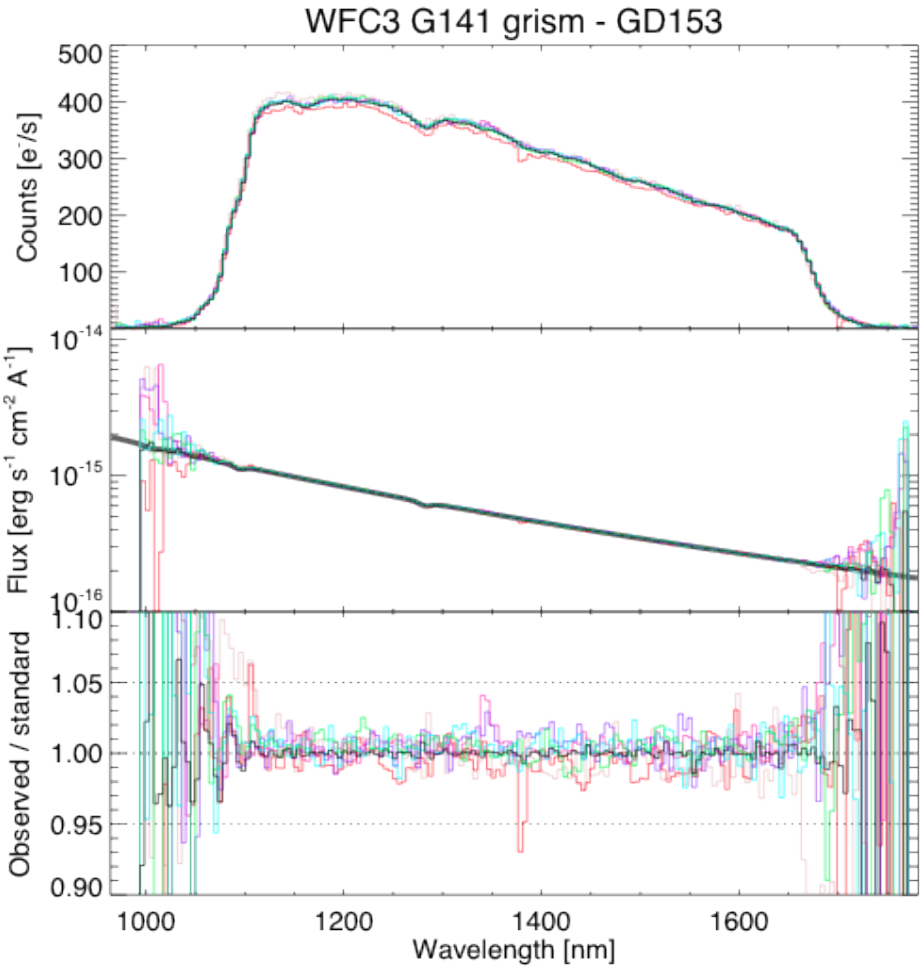

Figure 2: Flux calibration of the G141 grism. From top to bottom: The aXe extracted 1-dimensional spectra of the standard star GD153 in units of electrons per second per pixel, fully calibrated flux units and the ratio of the observed flux over the model spectrum versus wavelength. Observations obtained at different field positions are coloured, and the combined (aXedrizzle) central spectrum is shown in black.

A comparison with the previously published sensitivity curves (version 1.0; see Figure 3) reveals only minor (<2.5%) differences within the central wavelength range. Marked deviations, however, are seen towards the edges, where improved data reduction and background subtraction have the largest impact.

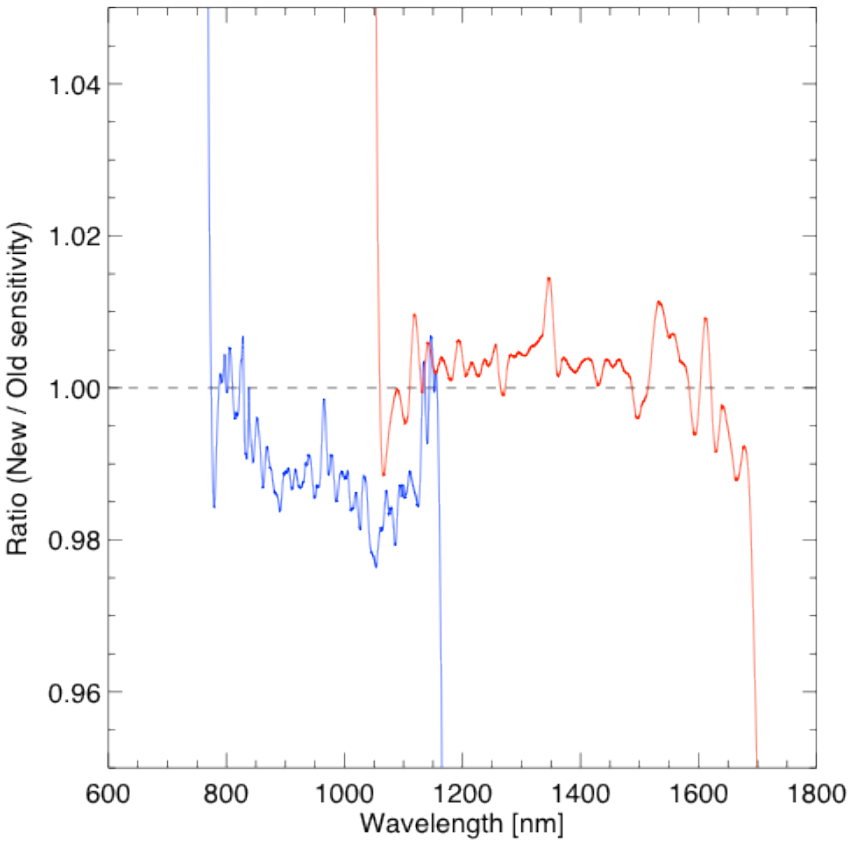

Figure 3: Ratio of sensitivity curves derived in this ISR and the previous version 1.0 (Kuntschner et al. 2009a,b). The blue and red lines represent the G102 and G141 grisms, respectively.

Sensitivity curves were also derived for the +2nd, +3rd and -1st orders. For the +2nd order we combined the four central exposures, whereas for the +3rd and -1st orders only one exposure was available. Due to the small dispersion, a calibration of the sensitivity curve for the 0th order from in-orbit data is very difficult and we rely here on the determinations from the last ground calibrations (Kuntschner et al. 2008). In future studies it may well be valuable to further explore the possibility of calibrating the 0th order from in-orbit data. In Figure 4 we summarize the total transmissions for both IR grisms. Note that this ISR presents sensitivity curves version 2.0 which are indicated in the calibration file names by a "*.sens.2.fits"; e.g. the sensitivity file for the +1st order of the G102 grism is **WFC3.IR.G102.1st.sens.2.fits**.

The peak throughput of HST + WFC3 G102 is 41% at 1100 nm, while it is >10% over the wavelength range 804 to 1153 nm. For G141 the peak throughput is 48% and throughput is above 10% for the wavelength range 1081 to 1691 nm.

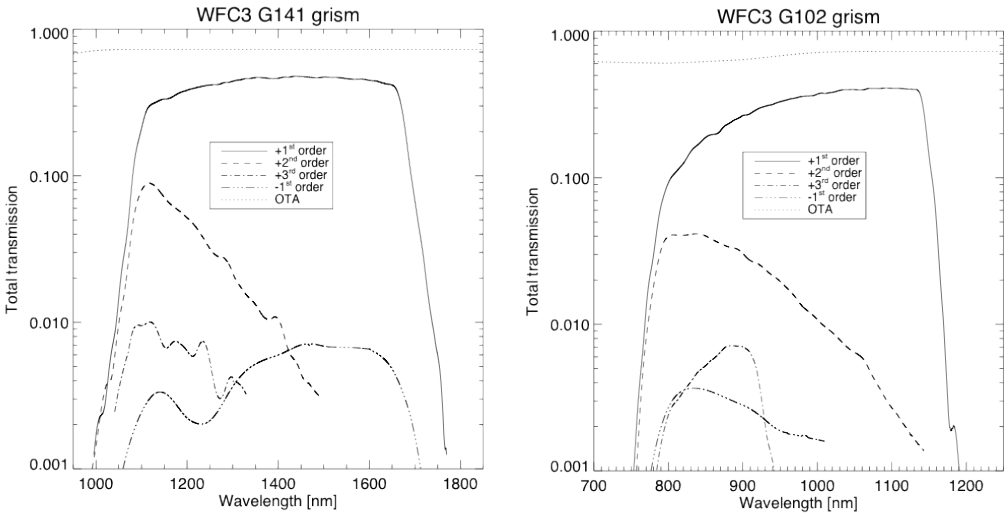

Figure 4: Total throughput estimates for the +1st, +2nd, +3rd and -1st orders of the G102 and G141 grisms, derived from the sensitivity curves determined in this report.

In Figure 5 we give an overview of the combined G102 and G141 total throughput showing also the overlap in wavelength for the two IR grisms. The wavelength ranges over which spectral extraction for science purposes is robust (throughput > 10%) is indicated: 803.5 – 1153.8 nm and 1080.6 – 1691.8 nm for G102 and G141, respectively. The throughput > 5% range, which is still useful for science extraction is 786.1 – 1159.8 nm and 1071.6 – 17062.0 nm for G102 and G141, respectively.

We emphasize that the flux calibrations presented in this report are only valid for point sources. For extended sources the size and shape of the object need to be taken into account (for more details see e.g. Freudling et al. 2008)

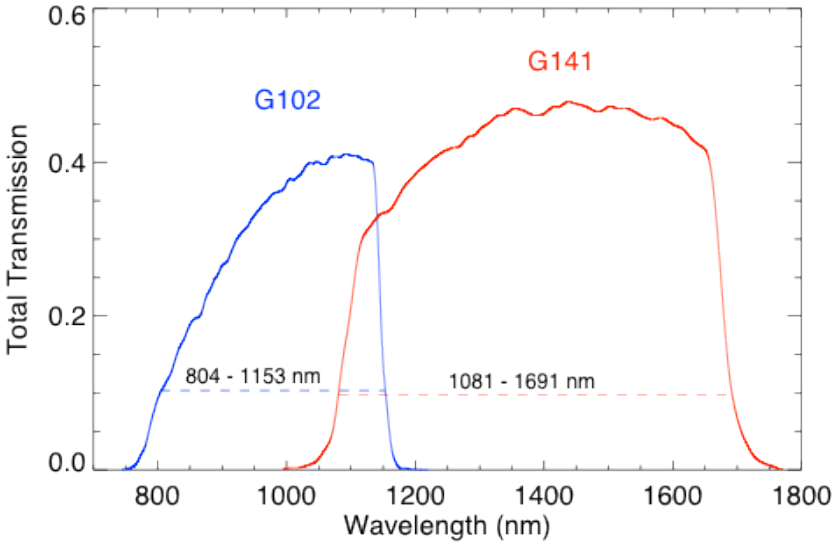

Figure 5: Overview of total transmission for the G102 and G141 grisms. The spectral ranges with more than 10% throughput are indicated.

In order to independently verify the validity of the flux calibration we made use of data from program 11936 obtained in Cycle 17. Here the flux standard star GD71 was observed for two telescope rotations and at 9 positions over the FoV. The central position consists of 4 independent dither steps. Using the observations for telescope orientation of ~275˚ (header keyword PA_V3), we reduced the data with standard configuration files and the flux curves described in this ISR for each grism. In the vicinity of GD71 there are several fainter stars visible, producing spectral traces in overlap with the $+1^{st}$ order spectrum of GD71. In order to minimize contamination, the extraction aperture was set to only ±3 pixels; the extracted spectra were corrected to an aperture of infinity by making use of the correction tables given in Section 3.2. Figure 6 presents the summary plots of the derived sensitivities for GD71.

The overall agreement is good with only individual field positions showing significant deviations (3-5%), likely caused by spectral overlap of neighboring, fainter stars. Evaluated over the wavelength range having >10% total throughput, the median ratio of the observed and model spectra is 1.006 and 1.005 for the G102 and G141 grisms, respectively. A robust estimate of the rms over the same wavelength range gives 1.5% and 1.7% for the G102 and G141 grisms, respectively. Therefore we conclude that for point sources the absolute flux calibration is accurate to 2% (one standard deviation) and better than 5% for almost the entire FoV.

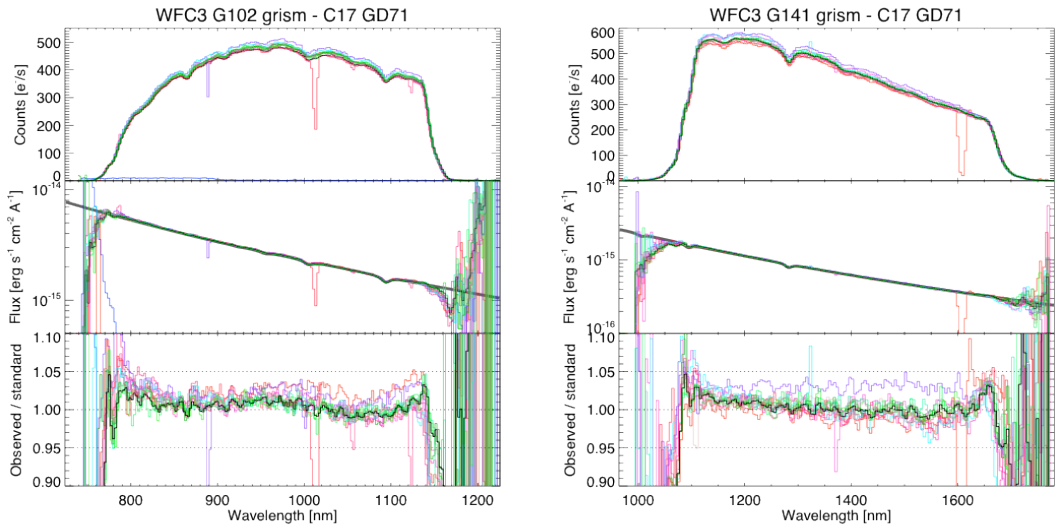

Figure 6: Overview of the reduction of flux standard star GD71 from Cycle 17 calibration proposal 11936 (HST orientation ~275°). Shown are (from the top to bottom) spectra in units of electrons per second per pixel, fully calibrated flux units and the ratio of the observed flux over the model spectrum versus wavelength. Spectra observed with the G102 and G141 grism are shown on the left and right, respectively. Different colours represent different positions within the FoV, while the black spectra show the central, drizzeled spectrum for each grism.

3.2. Aperture corrections

Using the aXe software (aXedrizzle option) we derived a rectified 2-dimensional image for the central exposures of the star GD153 for each grism. The resulting image (called a "stamp" image; type "*.mef_ID1.fits") is wavelength calibrated and image distortions, as recorded in our trace calibrations, are removed. From this image, which covers a 220 pixel wide aperture around GD153, various sub-apertures (here used in the sense of a diameter) were extracted using IDL scripts and compared to the flux one determines in the largest aperture. This procedure is carried out as a function of wavelength in five bins. The resulting aperture correction values are given in Tables 6a,b and shown graphically in Figure 7.

GD153 is an exceptionally isolated star and thus even for the largest aperture used in the above determinations we expect the contamination from neighboring stars to be negligible. Note that the aperture corrections given here are only applicable to point sources.

Table 6a: Aperture corrections for WFC3 G102

Diameter ["]	885 nm	935 nm	985 nm	1035 nm	1085 nm	1135 nm
0.128	0.459	0.391	0.414	0.464	0.416	0.369
0.385	0.825	0.809	0.808	0.811	0.794	0.792
0.641	0.890	0.889	0.887	0.880	0.875	0.888
0.898	0.920	0.917	0.916	0.909	0.904	0.916
1.154	0.939	0.937	0.936	0.930	0.925	0.936
1.411	0.952	0.950	0.950	0.943	0.940	0.949
1.667	0.962	0.961	0.961	0.954	0.951	0.958
1.924	0.969	0.968	0.969	0.962	0.959	0.965
3.719	0.985	0.984	0.986	0.982	0.980	0.983
7.567	0.995	0.995	0.996	0.991	0.990	0.992
12.954	0.999	0.999	0.999	0.997	0.996	0.995
25.779	1.000	1.000	1.000	1.000	1.000	1.000

Table 6b: Aperture corrections for WFC3 G141

Diameter ["]	1130 nm	1230 nm	1330 nm	1430 nm	1530 nm	1630 nm
0.128	0.442	0.444	0.395	0.344	0.342	0.376
0.385	0.805	0.792	0.764	0.747	0.732	0.732
0.641	0.886	0.877	0.865	0.863	0.850	0.859
0.898	0.912	0.901	0.893	0.894	0.884	0.898
1.154	0.933	0.924	0.914	0.913	0.903	0.913
1.411	0.947	0.940	0.931	0.932	0.921	0.932
1.667	0.958	0.950	0.942	0.944	0.934	0.945
1.924	0.966	0.959	0.951	0.953	0.944	0.954
3.719	0.985	0.984	0.981	0.985	0.980	0.985
7.567	0.993	0.995	0.992	0.997	0.992	0.996
12.954	0.996	0.998	0.997	1.000	0.997	1.000
25.779	1.000	1.000	1.000	1.000	1.000	1.000

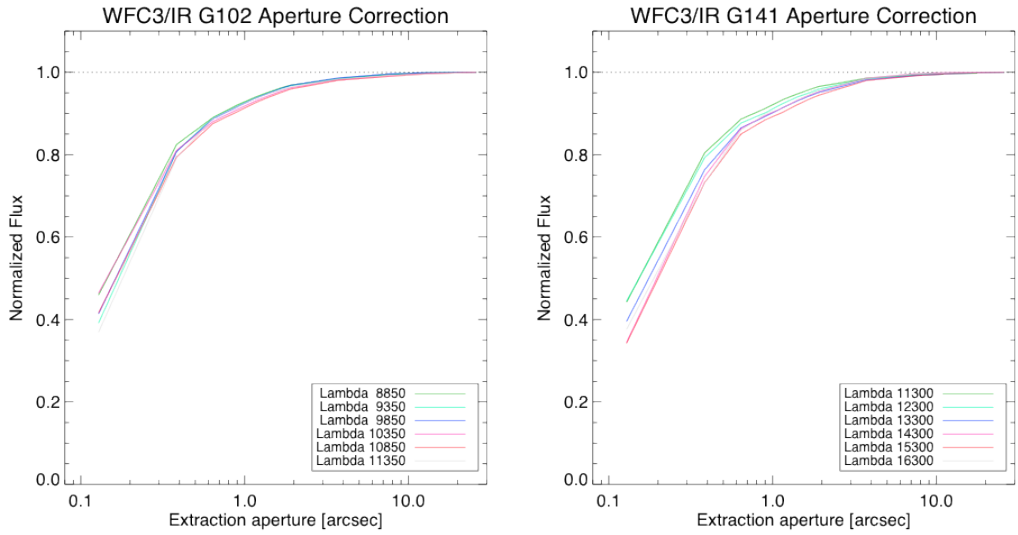

Figure 7: Aperture corrections for WFC3 G102 and G141 as a function of aperture (=diameter) and wavelength. The corrections are derived from observations of GD153 (Program 11552).

3.3. Large-scale grism throughput corrections

Similar to direct imaging, the WFC3 IR grisms show overall throughput variations as function of position in the FoV. Kuntschner et al. (2009a,b) reported that the throughput falls off from the center by about 5% for the off-center positions probed in Program 11552 (top left and bottom right). Using the observations of the flux standard star GD71 in Program 11936 (HST orientation ~90˚) we established relative throughputs for all 8 off-center field positions with respect to the central position. We did not find any significant difference between the two IR grisms and hence decided to fit a 2nd order surface (no cross-terms included) to the combined data points. The resulting fit can be seen in Figure 8. The maximum difference between any data point and the model-fit is 1.2% while the rms is 0.3%. This methodology was first developed for the ACS G800L grism; see Walsh and Pirzkal (2005) for details.

We confirm the earlier findings that the throughput falls off by about 2% in y-direction and by about 4% in x-direction to the edges of the FoV. In order to account for this large-scale variation we modified the 0th extension of the flat-field cube by simply multiplying the above described fitted surface into it. This will ensure that in any aXe data-reduction the large-scale throughput variations are taken care of in the flat-fielding process. The new flat field cubes are WFC3.IR.G102.flat.2.fits and WFC3.IR.G141.flat.2.fits.

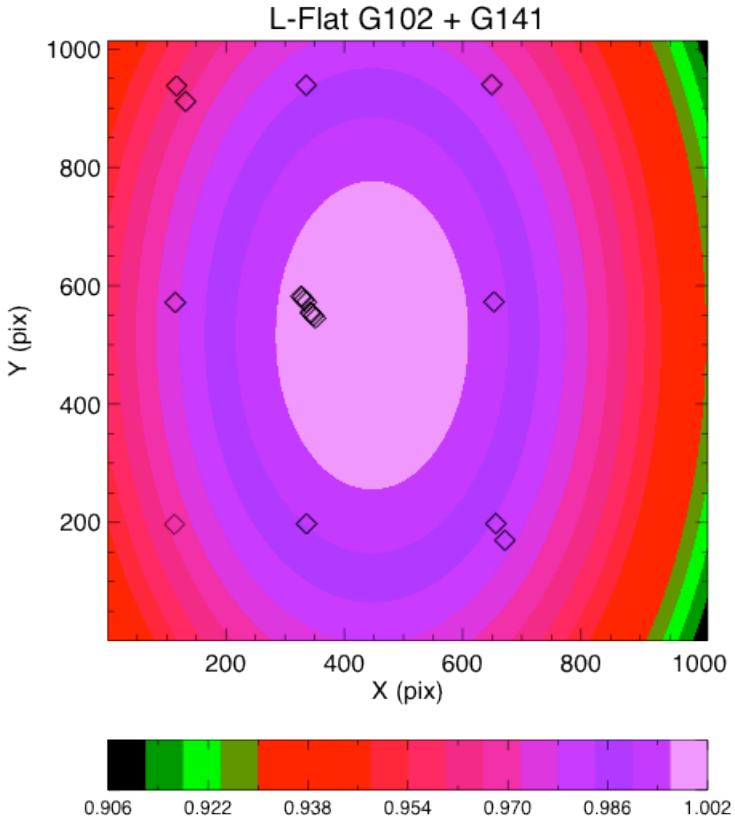

Figure 8: The overall shape of the large-scale throughput variations for the WFC3 IR grisms is shown. The colours represent a smooth 2nd order surface without cross-terms fitted to the individual throughput determinations for the flux standard star GD71 in the G102 and G141 grisms. The field positions of the target in direct imaging are shown as open diamonds (note that the centers of the +1st order spectra are shifted by about +100 pixel in x-direction).

4. Conclusions

This ISR presents revised flux calibrations for the WFC3 G102 and G141 grisms based on SMOV data (Program 11552; HST primary flux standard GD153) and verified with Cycle 17 observations (Program 11936; HST primary standard star GD71). We establish flux calibrations for the +1st, +2nd +3rd and -1st orders. The total throughput of HST + WFC3 G102 peaks at 1100 nm with 41% and is above 10% between 804 and 1153 nm. For G141 the total throughput peaks at 48% and is

above 10% between 1081 and 1691 nm. For the above 10% throughput wavelength range the accuracy of the absolute flux calibration for point sources is about 2% (one standard deviation) and better than 5% for most of the field-of-view. We also provide revised aperture corrections for the $+1^{st}$ order as a function of wavelength for each grism and determine the large-scale throughput variations for the grisms as a function of field-of-view position.

Calibration and reference files resulting from the data presented in this ISR are of version 2.0, which is indicated in the file names by "*.2.fits"; e.g. the sensitivity file for the $+1^{st}$ order of the G102 grism is **WFC3.IR.G102.1st.sens.2.fits**.

References

Freudling et al., 2008, A&A, 490, 1165: The Hubble Legacy Archive NICMOS grism data

Kümmel, M., Kuntschner H., Walsh, J. R., Bushouse, H., 2011, WFC3 Instrument Science Report, WFC3-2011-01: Master sky images for the WFC3 G102 and G141 grisms

Kuntschner, H. Bushouse, H., Kümmel, M., Walsh, J. R., 2009a, WFC3 Instrument Science Report, WFC3-2009-18: WFC3 SMOV proposal 11552: Calibration of the G102 grism

Kuntschner, H. Bushouse, H., Kümmel, M., Walsh, J. R., 2009b, WFC3 Instrument Science Report, WFC3-2009-17: WFC3 SMOV proposal 11552: Calibration of the G141 grism

Kuntschner, H. Bushouse, H., Walsh, J.R., Kümmel, M., 2008, WFC3 Instrument Science Report, WFC3-2008-16: The TV3 ground calibrations of the WFC3 NIR grisms

Walsh, J.R., Pirzkal, N. 2005, ACS Instrument Science Report ACS 2005-002: Flat-field and sensitivity calibration for ACS G800L slitless spectroscopy modes